

## Characterizing a Chip Scale Atomic Clock in Low Earth Orbit

Mikaela Dobbin, Austin Hunter, William Gravel, Conner Parker, Penina Axelrad  
 The University of Colorado Boulder  
 3775 Discovery Dr, Boulder, CO 80303  
[mikaela.dobbin@colorado.edu](mailto:mikaela.dobbin@colorado.edu)

### ABSTRACT

The University of Colorado Boulder has developed an experiment to characterize the behavior of a chip-scale atomic clock (CSAC) in space, conducted on the MAXWELL CubeSat mission. This experiment integrates a CSAC as an external oscillator to the onboard GPS receiver, enabling clock characterization through real-time estimates of clock bias, GPS pseudorange, and carrier phase measurements. These data will demonstrate the CSAC's short and long-term stability and its sensitivity to the space environment.

This paper evaluates the observation of CSAC performance using GPS within the constraints of the MAXWELL mission. The results, derived from tests with realistic orbit and spacecraft pointing scenarios modeled with an RF signal simulator and ground-based live-sky test data, show that poor GPS visibility limits CSAC observation accuracy and can result in data gaps. We demonstrate a gap-filling algorithm to effectively address these gaps. To mitigate the effects from poor visibility, GPS measurements from live-sky tests are processed with the GipsyX software suite to achieve the most accurate clock stability information. Since the MAXWELL receiver operates at a single frequency and is susceptible to ionospheric effects, we apply the Group and Phase Ionospheric Correction (GRAPHIC) technique to mitigate first-order ionospheric effects for GPS-based clock characterization in Low Earth Orbit (LEO).

### INTRODUCTION

Accurate and stable timing is important for many satellite operations. Nearly all Earth-orbiting satellites rely on Global Navigation Satellite Systems (GNSS), and primarily the U.S. Global Position System (GPS), for positioning and timing. GNSS satellites are equipped with high-precision atomic clocks that generate excellent reference signals, enabling accurate estimates of satellite positions and onboard clock error.

In situations when GPS signals are unavailable, such as during temporary outages caused by signal interference or jamming, or when a satellite is operating in deep space far beyond the reach of GPS coverage, it is important to have a reliable and stable onboard. This helps to ensure that accurate satellite navigation and timing are maintained. Furthermore, the inclusion of a stable, onboard timing reference allows for improved spacecraft autonomy and can reduce the reliance on ground station support.<sup>1</sup>

However, the current state-of-the-art clocks onboard GNSS satellites and flagship deep space missions are impractically large and heavy for use on small satellites. As more satellites adopt smaller form factors, such as SmallSats and CubeSats, there is a growing need for accurate and stable timing references

that meet the size, weight, and power constraints of smaller platforms.

Chip-scale atomic clocks (CSACs) are a promising solution, as they require only a small fraction of the size, weight, and power of oscillators used in GNSS satellites. Figure 1 depicts a CSAC with a quarter for size reference. However, as a relatively new technology, CSACs have yet to be extensively tested and characterized in spaceborne applications. Most recently, the CHOMPPT CubeSat mission reported its results measuring the on-orbit performance of a CSAC through optical time transfer in 2023.<sup>2</sup> Their results show on-orbit performance of the CSAC is consistent with pre-flight ground testing.<sup>2</sup>



Figure 1: Microchip SA .45 CSAC<sup>3</sup>

With the goal of observing CSAC performance in an orbital environment, the University of Colorado Boulder has developed a dedicated experiment that will be performed onboard the Air Force Research Lab (AFRL) University Nanosatellite Program (UNP-9) MAXWELL CubeSat mission. During the experiment, a CSAC will be used as an external oscillator for the onboard GPS receiver to measure the clock stability, a well-established technique for observing clock performance on the ground. The experiment will be conducted over a period of five days, logging measurements of pseudorange, carrier phase, clock bias, and satellite position. Telemetry data from the CSAC, such as temperature, will also be logged to assess how thermal variations in the space environment impact the CSAC performance. The recorded data will be downlinked via an X-band antenna and processed to evaluate the stability of the CSAC in LEO.<sup>4</sup>

This paper assesses our ability to observe CSAC performance using GPS under the constraints of the MAXWELL mission. An RF simulator is used to produce high-doppler signals and GPS satellite visibility observed in LEO. Within the simulator, we model both zenith and sun-pointing modes to investigate the how limited GPS visibility influences the accuracy of GPS-based clock solutions. Additionally, live-sky test data is used to demonstrate processing methods using carrier phase measurements from the receiver in post-processing to improve our observations of clock performance.

## CSAC EXPERIMENT OVERVIEW

MAXWELL (Multiple Access X-Band Wave Experiment Located in LEO) is a 6U CubeSat mission designed and built at the University of Colorado under AFRL’s University Nanosat Program. The primary goal of this mission is to demonstrate high-rate RF communication technology, specifically through an S-band uplink and X-band downlink.<sup>4</sup>

The CSAC experiment is one of MAXWELL’s secondary objectives to be conducted after the primary communication demonstrations. This experiment utilizes a GPS receiver that supports external clock input. With the received signals from a minimum of four satellites, a GPS receiver solves for three components of position and the offset of the external clock relative to GPS. This estimation of clock offset, or bias facilitates the observation of the accuracy and stability of the external clock input, benchmarked against the highly accurate GPS reference signal.

Figure 2 illustrates the block diagram for the CSAC experiment. A Microchip SA.45 CSAC signal serves

as a 10 MHz oscillator input for a NovAtel OEM729 GPS receiver. The GPS radio frequency (RF) input comes from a single frequency (L1 only) antenna. Single frequency was chosen due to cost and power constraints on the mission. Both the CSAC and the GPS receiver are controlled by the MAXWELL flight computer, which also logs CSAC telemetry and GPS measurements, to the flight computer.

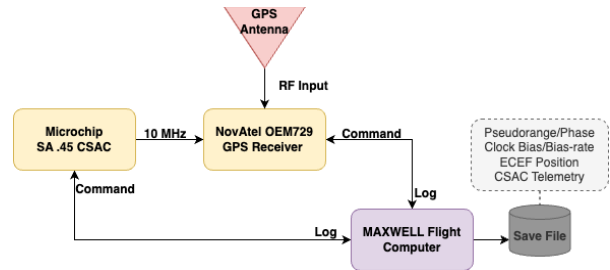


**Figure 2: CSAC flight experiment block diagram**

## Clock Characterization & Frequency Stability

To characterize clock stability, we consider the consistency of frequency over different time intervals. This is achieved by comparing the timing or phase of the clock to a more accurate reference signal. In the CSAC experiment, the GPS signals observed by the receiver serve as this reference. The CSAC bias relative to GPS time and its bias rate show up in receiver observations and are explicitly determined in its real-time solution. For an undisciplined oscillator like the CSAC, the bias is expected to increase at a nearly constant rate, indicating a gradual drift out of synchronization with GPS time.<sup>3</sup>

Clock stability is evaluated by analyzing the detrended clock bias, which highlights the deviations from the constant bias rate. These detrended values are used to compute the Allan Variance, or its square root, the Allan Deviation (ADEV), which quantifies frequency stability over a range of averaging intervals. Lower ADEV values indicate a more stable clock. Figure 3 depicts an example of an ADEV plot, indicating the slopes and sections corresponding to the types of noise typically seen across varying averaging intervals.

The advantage to using GPS to measure clock stability is that it allows us to observe the CSAC performance continuously over a complete range of averaging intervals. This is valuable because we gain insights of the precision of the CSAC at short intervals ( $\tau < 10$  seconds) as well as its stability at longer intervals ( $\tau > 100$  seconds).

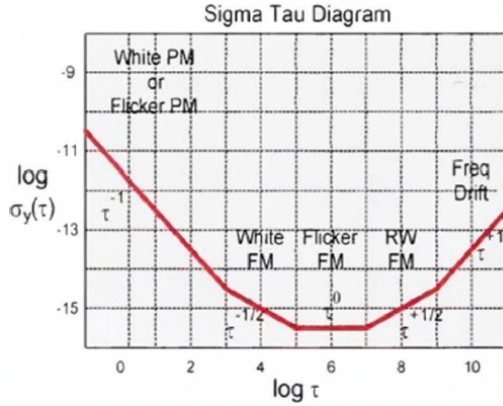


Figure 3: Example of an ADEV plot from Riley (2008).<sup>8</sup>

### CSAC TESTING

To prepare for the CSAC flight experiment, ground tests under different conditions have been conducted to establish baseline expectations for the CSAC performance in orbit. These tests use the same setup shown in Figure 2, but rather than logging to the flight computer, the data is logged directly to a computer via USB. Previous tests placed the CSAC into a thermal chamber to simulate and evaluate the impact of the variable thermal environment expected in orbit.<sup>6,7</sup> The influence of changing magnetic fields on CSAC behavior, due to the proximity of torque rods, was also studied.<sup>7</sup> Both investigations used RF input from an outdoor antenna. Additionally, preliminary simulations using Satellite Tool Kit (STK) were developed to study the on-orbit visibility of GPS satellites.<sup>5</sup> Early tests were also conducted using an RF simulator to verify acquisition and tracking of high Doppler signals expected in LEO.<sup>6</sup>

The results presented in this paper utilize two sources of GPS RF input: **live sky** from a rooftop GPS antenna connected to the NovAtel receiver and **RF simulated** from a Spirent GPS simulator. Both live sky and RF simulator configurations offer distinct advantages. Live sky testing provides real-world GPS signals, ensuring that the receiver and external clock configuration can successfully process authentic satellite signals and deliver accurate clock estimates. It also allows testing under real environmental conditions, including atmospheric effects, which can influence clock estimates, especially for single-frequency receivers. On the other hand, an RF simulator offers a controlled environment that enhances the repeatability of tests. The simulator gives us the ability to test the receiver hardware and software that will be used during the experiment. Additionally, the simulator can model various spacecraft pointing modes, allowing us to collect realistic data on on-orbit

GPS satellite visibility and signal strength. This enables us to evaluate the impact on observations of CSAC performance.

### RF SIMULATOR SCENARIO

RF simulator testing is conducted to evaluate the expected performance of the CSAC experiment in an orbit scenario with high Doppler shifts and GPS visibility constraints based on the type of orbit and spacecraft pointing. The simulator results presented in this paper were obtained using a Spirent GSS9000 RF simulator, with the scenario parameters listed in Table 1.

Table 1: RF Simulator Scenario Parameters

Description	Value
Epoch Date	13 November 2023
Orbital Altitude	500 km
Inclination	60 degrees
Eccentricity	0
Vehicle Mass	14 kg
Reference Area	0.06 m <sup>2</sup>
Reflection Coefficient	1.3

The simulator also accepts a user antenna pattern, for which we use the Maxwell GPS antenna gain pattern. The antenna exhibits maximum gain at the top, which gradually decreases to maximum attenuation to simulate the spacecraft body obstructing GPS signals. We also note that the ionospheric models within the simulator are disabled.

Two pointing modes are modeled with the simulator. The first is the zenith-pointing mode, where the antenna is always oriented away from the Earth. This mode is optimal for the experiment as it maximizes the visibility of GPS satellites, resulting in better position and clock solutions. The second mode is the sun-pointing mode, where the antenna is oriented towards the Sun. This mode is considered because MAXWELL was designed with the GPS antenna and solar panels mounted on the same surface. To maintain positive power, the spacecraft will often operate in a sun-pointing mode, which may limit GPS satellite visibility. For example, if the Sun is fully eclipsed by the Earth, very few GPS satellites will be in view, potentially resulting in data gaps. Although it is unlikely that MAXWELL will operate in a sun-pointing mode when the Sun is not visible, considering this worst-case scenario clarifies how to gather useful data during data outages.

### Simulator Solution Verification

To verify that the receiver computes accurate position solutions within the simulated scenario, its position solutions are compared to the true positions provided by the simulator. Figure 4 illustrates the position errors of the NovAtel OEM729 receiver using the simulator scenario described in Table 1 in a zenith-point mode. The receiver solutions are within 1 meter RMS of the truth, with the lowest errors corresponding to times when more satellites are in view.

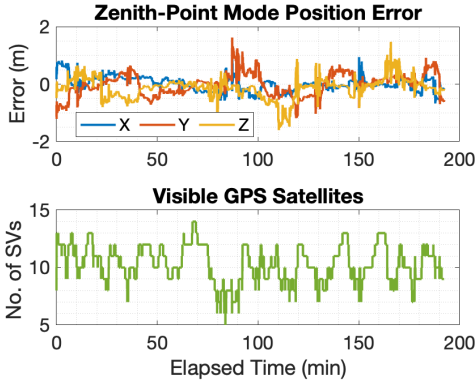


**Figure 4: NovAtel position solution errors from RF simulator zenith-pointing scenario**

The instantaneous clock bias and detrended bias for the same zenith-pointing scenario, are plotted in Figure 5 with the ADEV of the detrended bias shown in Figure 6. The stability performance specifications of the Microchip SA.45 CSAC are also included for reference.<sup>3</sup> We see in Figure 6 that the ADEV from the zenith-pointing mode is lower than the CSAC specification, indicating that this CSAC used in testing is more stable than the manufacture’s expectation.

### SIMULATING LIMITED GPS VISIBILITY

The MAXWELL GPS antenna is mounted on the same surface as the spacecraft’s solar panels, causing the spacecraft to spend significant portions of its orbit in a sun-pointing mode. Using the scenario parameters detailed in Table 1, we programmed the Spirent simulator to produce GPS signals for a spacecraft operating in this mode, where the antenna boresight points towards the Sun. This orientation results in intervals with fewer satellites in view, leading to less accurate position and clock solutions. Figure 7 shows a plot of the number of satellites visible in the sun-pointing mode, and the number of satellites visible in the zenith-point mode included for reference.

Real-time point solutions require signals from a minimum of four GPS satellites to obtain a 3D-position and clock solution. When there are fewer

signals available, the receiver still logs individual satellite measurements but does not report a solution. Thus, we see in Figure 7 that there are instances in the sun-pointing scenario that fewer than four satellites are in view, resulting in clock solution gaps. We also note that as more satellites are in view, there are more measurements available and the uncertainty in the clock solution is reduced.

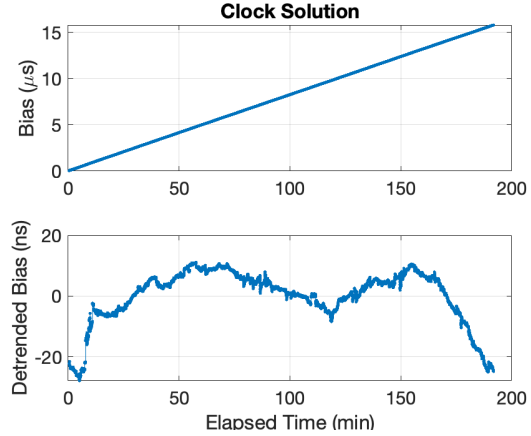


**Figure 5: Clock solutions from zenith-pointing RF simulator scenario**

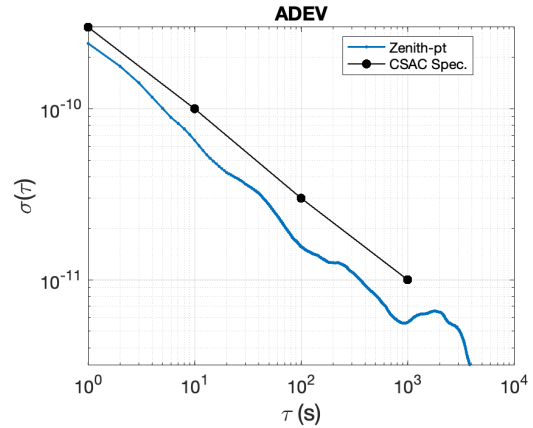


**Figure 6: ADEV of zenith-pointing clock solution with CSAC specification as reference**

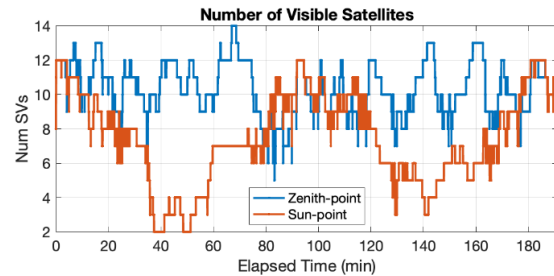


**Figure 7: Comparison of number of visible satellites for zenith and sun-pointing scenarios**

### Sun-Pointing Clock Solutions

To compute frequency stability, the time-series data must be equally spaced. To account for gaps caused by the limited GPS visibility in sun-pointing mode, we segment the data into continuous sections for individual analysis. This gives good results for short intervals but makes it challenging to characterize the CSAC's long-term stability. Figure 8 shows the clock solution from the sun-pointing mode, highlighting where clock solution gaps exist (shown in grey) and where adequate continuous clock solutions can be computed (shown in color). Data gaps occur when fewer than four satellites are in view or have insufficient signal strength to be tracked, resulting in four segments of continuous data over a 5-hour test period. Figure 9 shows the ADEVs computed from each segment, including the ADEV from the zenith-pointing scenario and CSAC specification for reference.

Looking at Figure 9, we notice that at short intervals (averaging time,  $\tau$ , from 1 to 10 seconds) there are substantial differences between the segments, with only one of the four showing an ADEV below the CSAC. Given that the zenith pointing results showed results consistently below the specification, we can conclude that in the sun-pointing mode, the poor quality of the GPS point solutions is hampering our ability to observe the true behavior of the CSAC. This is one of the motivations for the enhanced post-processing method described in the next section.

### Data Gap Filling

In addition to analyzing individual segments of continuous data, the data gaps may also be filled. This approach is particularly useful for instances on orbit where unpredictable data outages may further limit the usable time history for measuring clock stability. We implement the gap-filling method detailed by Howe & Schlossberger.<sup>9</sup> This algorithm fills gaps by imputing an extension of the real data into the gap by reflecting it about its end, then matching the phase slope to align with the following segment.<sup>9</sup>

Figure 10 shows the resulting bias and detrended bias from the sun-pointing scenario after implementing the gap-filling algorithm.<sup>10</sup> The segmented data time histories were augmented and detrended as a single dataset, resulting in the lighter blue line shown in Figure 10. The detrended results were then processed through the gap-filling algorithm, yielding the connecting data shown in the darker blue.

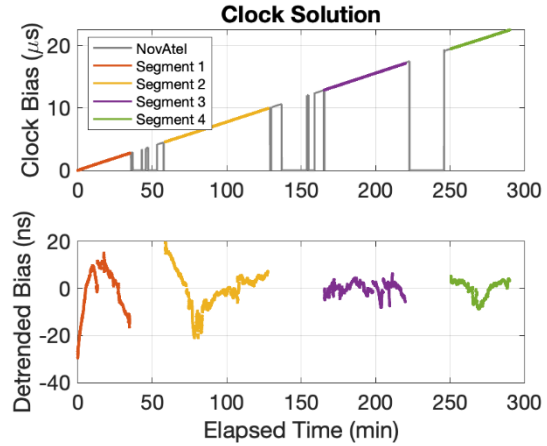


Figure 8: NovAtel clock solution from RF simulator sun-pointing scenario

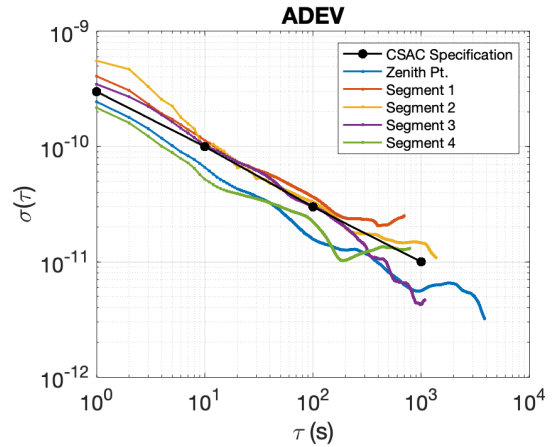


Figure 9: ADEVs of detrended clock solutions from sun-pointing scenario with CSAC spec and zenith-pointing for comparison (Figure 8)

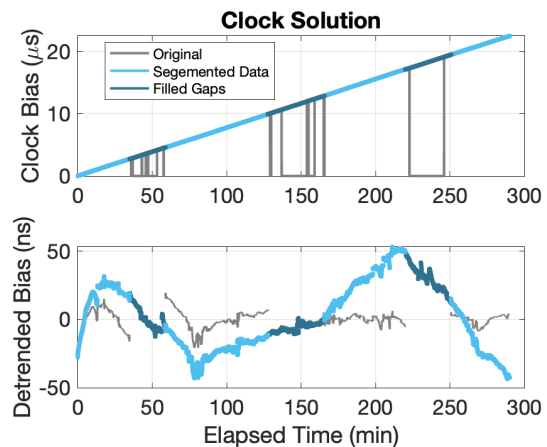
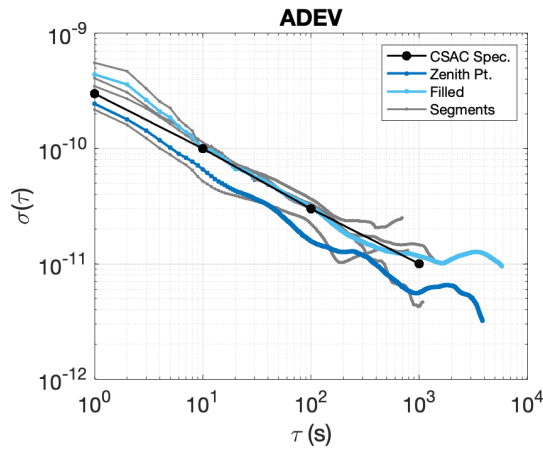


Figure 10: Demonstration of gap filling algorithm on clock solution from sun-pointing scenario

The complete time history of the detrended bias, shown in Figure 10, is used to compute ADEV presented Figure 11. The grey lines in the figure represent the ADEVs computed from the individual data segments. It is evident that the gap-filling process does not introduce additional noise or instability in the ADEV, maintaining the clock stability observed in the individual segments. Once again, it is apparent that even with the gaps filled, we are still limited by the number of satellites in view to obtain accurate clock observations, motivating additional processing methods to better recover the CSAC performance.



**Figure 11: ADEV of detrended clock bias with gaps filled from sun-pointing scenario**

### LIVE SKY TESTING

Live sky testing supports processing of real GPS signals, allowing for the verification of expectations and refinement of post-processing techniques. Although live sky test results do not replicate the satellite geometry or spacecraft dynamics experienced in orbit, they are invaluable for establishing expected clock performance and stability. Additionally, this approach allows for the evaluation of atmospheric effects not currently modeled in the simulator. While multipath and atmospheric effects, such as ionospheric delays, differ on the ground compared to in orbit, live sky testing helps develop and test mitigation methods transferable to the orbital context. These tests also facilitate the implementation of advanced post-processing techniques that cannot be applied to simulated data due to dependencies on real, high-precision data.

The setup for the live sky test is similar to the simulator configuration. However, instead of using the RF input from the simulator, we get the RF input from a rooftop antenna cabled into the lab for receiver testing.

### Single-frequency Receiver

As mentioned earlier, the NovAtel OEM729 receiver intended for use on MAXWELL is single-frequency. This precludes the use of dual-frequency corrections typically employed on scientific satellite missions. Parametric empirical models for ionospheric delays on GPS to LEO signals are not very accurate, and for the expected altitude of MAXWELL, our default approach is to turn off the simple ionospheric corrections. Figure 12 demonstrates the effect of unmodelled ionospheric effects on ground-based clock solutions, using the same CSAC and GPS RF signals input to both a dual-frequency and a single-frequency receiver. The solutions are very similar, with the lower subplot showing that the differences are well within 10 nanoseconds.

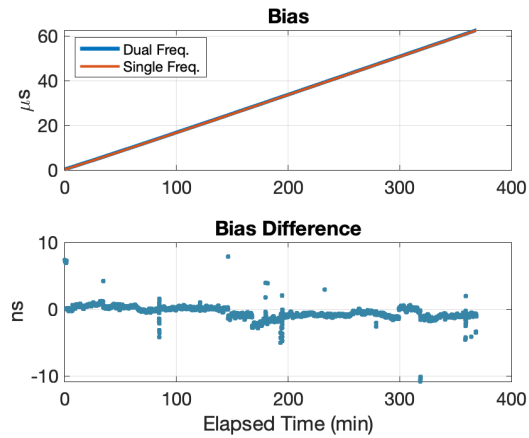


**Figure 12: Comparison of dual and single-frequency receiver clock solutions from live sky test**

Based on these results, the use of a single-frequency receiver is not expected to significantly impact the clock solutions when compared to dual-frequency receiver. Nonetheless, additional post-processing techniques are considered in the following section to further mitigate any potential ionospheric effects and improve clock solutions.

### Carrier Phase-Based Solutions using GipsyX

GipsyX, developed by NASA's Jet Propulsion Laboratory, is a software suite capable of computing highly accurate carrier-phase-based estimates of the receiver clock. The software utilizes precise orbit determination products for all GPS satellites, high-fidelity dynamic models, and accurate GPS antenna calibration maps.<sup>11</sup> Figure 13 and Figure 14 compare the results from a live sky test processed through GipsyX using both dual and single-frequency measurements to the instantaneous clock bias output from the NovAtel receiver. Although it is challenging

to distinguish between the NovAtel and GipsyX clock bias and detrended bias results in the time series plots, a significant improvement is observed in the ADEV, where the GipsyX results are lower in value. This outcome highlights errors in the instantaneous clock solutions caused by orbit errors, atmospheric delays, and multipath effects. It is also observed that the single-frequency and dual-frequency results are still nearly identical, further proving the negligible differences between single and dual-frequency solutions from live sky test data. Furthermore, we see that the ADEV of the NovAtel solutions agree with the GipsyX results at longer averaging intervals. This indicates that the long-term stability observations from the NovAtel clock solutions are accurate.

Compared to the CSAC performance reported from the CHOMPTT mission, our ADEV values at 100 seconds are consistent with their observations.<sup>2</sup> However, they achieve minimum variation (i.e., lowest ADEV value) in both their ground tests and on-orbit results at a shorter averaging interval than we observe.

### *Ionosphere-Free Single-frequency Measurements*

If ionospheric delays prove to be more significant in orbit than observed on the ground, a processing technique called GRAPHIC can be employed to eliminate ionospheric effects using single-frequency data<sup>12</sup>. The GRAPHIC method computes the mean single-frequency measurements as follows:

$$\rho = r + b + I + \varepsilon_\rho \quad (1)$$

$$\phi = r + b - I + N + \varepsilon_\phi \quad (2)$$

$$GRAPHIC = \frac{\rho + \phi}{2} = r + b + \frac{N}{2} + \frac{\varepsilon_\rho}{2} + \frac{\varepsilon_\phi}{2} \quad (3)$$

Where  $\rho$  is the pseudorange,  $r$  is range,  $b$  is clock bias,  $I$  is the ionospheric delay,  $\varepsilon$  is unmodeled errors,  $\phi$  is the carrier phase, and  $N$  are the integer ambiguities. Thus, GRAPHIC produces an ionosphere-free, phase-like observable.<sup>13</sup> To separate the clock and integer ambiguities, the raw, undifferenced pseudorange measurements anchor the clock solution, albeit de-weighted to minimize impact on the final position and clock solution. These measurements are input to GipsyX, which resolves the integer ambiguities and produces an accurate, ionosphere-free clock solution. Figure 13 and Figure 14 also include the GRAPHIC solutions processed using GipsyX. It is noted that since the single-frequency results are already closely aligned with the dual-frequency solutions without any significant ionospheric delay impact, the GRAPHIC

solution agrees with both the dual- and single-frequency outputs.

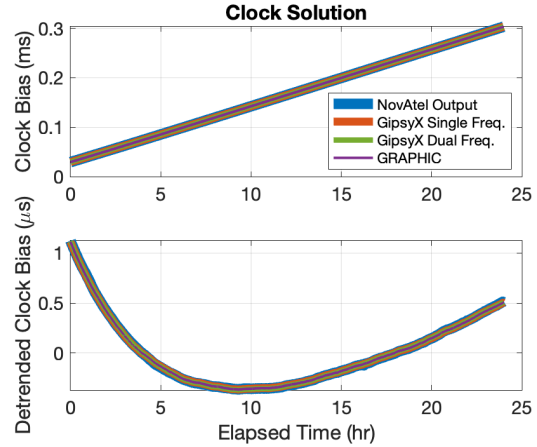


**Figure 13: Comparison of clock solutions from single-frequency, dual-frequency, and GRAPHIC processed with GipsyX with NovAtel solution**

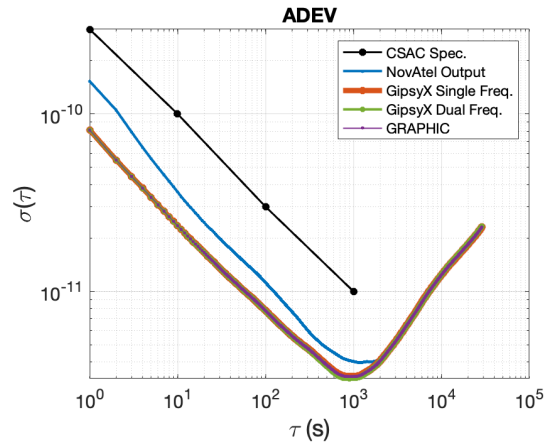


**Figure 14: Comparison of ADEVs from single-frequency, dual-frequency, and GRAPHIC solutions processed with GipsyX with NovAtel solution**

## CONCLUSIONS

In conclusion, this work aimed to evaluate our ability to observe CSAC on-orbit performance within the constraints of the MAXWELL mission. We demonstrated the effective use of an RF simulator to replicate GPS visibility constraints arising from various spacecraft pointing modes. Our findings indicate that limited GPS visibility can lead to data gaps, hindering accurate measurement of CSAC performance. To address this, we implemented a data-filling algorithm that successfully fills gaps while

maintaining clock characteristics, enabling evaluation of longer-term clock performance.

Through live sky testing and advanced post-processing techniques using GipsyX, we investigated the impact of single versus dual frequency receivers. Ground-based live sky evaluations revealed no substantial differences. However, considering potential ionospheric influence in orbit, we integrated GRAPHIC to rectify ionospheric delays in clock solutions.

In preparation for the MAXWELL launch and CSAC experiment, we anticipate obtaining the most accurate clock observations when the spacecraft is zenith-pointing. Nevertheless, in instances of limited GPS visibility, we are optimistic about leveraging carrier phase measurements and GipsyX to enhance results and plan to explore this in future research.

#### **Acknowledgements**

We would like to acknowledge past and current members of the CONTACT and MAXWELL teams at the University of Colorado Boulder for their contributions to the CSAC experiment.

#### **References**

1. M. Rybak, P. Axelrad and J. Seubert, "Investigation of CSAC Driven One-Way Ranging Performance for CubeSat Navigation," in *Conference on Small Satellites*, Logan, Utah, 2018.
2. T. Ritz, D. Coogan, J. W. Conklin, J. T. Coffaro, P. Serra, S. Nydam, J. Hanson, A. N. Nguyen, C. Priscal, J. Stupl and A. Zufall, "Laser time-transfer facility and preliminary results from the CHOMPTT CubeSat mission," *Advances in Space Research*, no. 71, pp. 4498-4520, January 2023.
3. Microchip, "SA.45s CSAC Datasheet 900-00744-000 Rev E," 2024. [Online]. Available: <https://www.microchip.com/en-us/product/csac-sa45s>.
4. MAXWELL, "Our Mission," 2020. [Online]. Available: <https://www.colorado.edu/project/maxwellcubesat/our-mission>.
5. Y. Khatri, P. A. Aboaf, D. Dowd, C. Flood, H. Dixon and P. Axelrad, "CSAC Flight Experiment to Characterize On-Orbit Performance," in *Small Satellite Conference*, Logan, Utah, 2020.
6. L. Schement and C. Dixon, "Ground Testing of a Chip-Scale Atomic Clock for MAXWELL CubeSat Flight Experiment," in *35th Annual Small Satellite Conference*, Logan, Utah, 2021.
7. M. Dobbin, C. Colpaert, C. Krebs and P. Axelrad, "Characterizing CSAC Performance in a Simulated Mission Environment," in *AAS GN&C Conference*, Breckenridge, Colorado, 2022.
8. W. J. Riley, *Handbook of Frequency Stability Analysis*, Boulder, Colorado: NIST Special Publication, 2008.
9. D. A. Howe and N. Schlossberger, "Characterizing Frequency Stability Measurements Having Multiple Data Gaps," *IEEE Transactions on Ultrasonics, Ferroelectrics, and Frequency Control*, vol. 69, no. 2, pp. 468-472, 2022.
10. N. Schlossberger and C. Champagne, "Time Series Imputation," GitHub, [Online]. Available: <https://github.com/nkschlos/time-series-imputation/tree/main>.
11. W. Bertiger, Y. Bar-Sever, A. Dorsey, B. Haines, N. Harvey, D. Hemberger, M. Heflin, W. Lu, M. Miller, A. W. Moore, D. Murphy, P. Ries, L. Romans, A. Sibois, A. Sibthorpe, B. Szilagyi and Vallisneri, "GipsyX/RTGx, a new tool set for space geodetic operations and research," *Advances in Space Research*, vol. 66, no. 3, pp. 469-489, 2020.
12. H. Bock, A. Jäggi, R. Dach, S. Schaer and G. Beutler, "GPS single-frequency orbit determination for low Earth orbiting satellites," *Advances in Space Research*, vol. 43, no. 5, pp. 783-791, 2009.
13. A. V. Conrad, P. Axelrad, B. Haines, C. Zuffada and A. O'Brien, "Improved GPS-Based Single-frequency Orbit Determination for the CYGNSS Spacecraft Using GipsyX," *Navigation*, vol. 70, no. 1, 2022.